

The Dakhleh Glass: Product of an impact airburst or cratering event in the Western Desert of Egypt?

Gordon R. OSINSKI^{1*}, Johanna KIENIEWICZ², Jennifer R. SMITH³, Mark B. E. BOSLOUGH⁴, Mark ECCLESTON⁵, Henry P. SCHWARCZ⁶, Maxine R. KLEINDIENST⁷, Albert F. C. HALDEMANN⁸, and Charles S. CHURCHER⁹

¹Departments of Earth Sciences/Physics and Astronomy, University of Western Ontario, London, ON N6A 5B7, Canada

²Department of Geosciences, Denison University, Granville, Ohio 43023, USA

³Earth and Planetary Sciences, Washington University, Campus Box 1169, One Brookings Drive, Saint Louis, Missouri 63130, USA

⁴Sandia National Laboratories, P.O. Box 5800, Albuquerque, New Mexico 87185, USA

⁵Archaeology Program, La Trobe University, Bundoora 3086, Australia

⁶School of Geography and Earth Sciences, McMaster University, Hamilton, ON L8S 4K1, Canada

⁷Department of Anthropology, University of Toronto at Mississauga, 3359 Mississauga Road North, Mississauga, ON L5L 1C6, Canada

⁸European Space Agency, ESTEC HME-ME, P.O. Box 299, 2200 AG, Noordwijk ZH, The Netherlands

⁹Department of Zoology, University of Toronto, Toronto, ON M5S 3G5, Canada

Corresponding author. E-mail: gosinski@uwo.ca

(Received 04 September 2008; revision accepted 31 December 2008)

Abstract—Impact cratering is a ubiquitous geological process on the terrestrial planets. Meteorite impact craters are the most visible product of impact events, but there is a growing recognition that large aerial bursts or airbursts should occur relatively frequently throughout geological time. In this contribution, we report on an unusual impact glass—the Dakhleh Glass (DG)—which is distributed over an area of ~400 km² of the Dakhleh Oasis, Egypt. This region preserves a rich history of habitation stretching back to over 400,000 years before the emergence of *Homo sapiens*. We report on observations made during recent fieldwork and subsequent analytical analyses that strengthen previous suggestions that the DG formed during an impact event. The wide distribution and large size of DG specimens (up to ~50 cm across), the chemistry (e.g., CaO and Al₂O₃ contents up to ~25 and ~18 wt%, respectively), the presence of lechatelierite and burnt sediments, and the inclusion of clasts and spherules in the DG is inconsistent with known terrestrial processes of glass formation. The age and other textural characteristics rule out a human origin. Instead, we draw upon recent numerical modeling of airbursts to suggest that the properties of DG, coupled with the absence of a confirmed crater, can best be explained by melting of surficial sediments as a result of a large airburst event. We suggest that glass produced by such events should, therefore, be more common in the rock record than impact craters, assuming that the glass formed in a suitable preserving environment.

INTRODUCTION

Meteorite impact structures are the dominant geological landform on many planetary bodies—such as the Moon, Mercury, and large parts of Mars—while Earth’s active tectonic and surface processes tend to rapidly erase impact structures from the geological record, so that only a fraction of the total population remains. The impact of comet Shoemaker-Levy 9 with Jupiter in 1994, however, demonstrated to the scientific community that large impact events in the solar system are not a thing of the geological past. The frequency of large impacts on Earth is much lower than on Jupiter and those with the potential for long-term global environmental effects (i.e., tens of millions of years; Shoemaker 1983) is such that meteorite

impacts are unlikely to have significantly affected the physical or cultural evolution of our species. However, over the past few years there has been a growing speculation that smaller, more frequent, impact events with significant regional effects may have substantially disrupted or influenced local human populations (Masse 2007). It is of note that, to date, little evidence of such impacts is recognized in inhabited regions and the size-frequency relation of near-Earth objects (Harris 2008) suggests that such events should have been extremely rare during the span of human history.

Meteorite impact craters are the most visible product of hypervelocity impact events. They form when a projectile is large and coherent enough “to penetrate the Earth’s atmosphere with little or no deceleration and to strike the

ground at virtually its original cosmic velocity (>11 km/s) (French 1998). At smaller diameters, the projectile is slowed down by passage through the Earth's atmosphere and so-called "penetration craters" are formed (e.g., the Sikhote-Alin crater field in Russia, formed from a meteorite shower in 1947). However, the impact of comet Shoemaker-Levy 9 with Jupiter also demonstrated the destructive potential of impact airbursts; no crater formed during this event because Jupiter lacks a solid surface. The 1908 Tunguska event represents the largest recorded example of an airburst event on Earth to date (Vasilyev 1998), with an estimated magnitude estimates ranging from 3 to 5 Mt (Boslough and Crawford 1997) up to ~ 10 –40 Mt. However, theoretical calculations coupled with ground- and satellite-based observations of airbursts suggest that the Earth is struck annually by a objects of energy 2–10 kt with Tunguska-size events occurring once every 1000 years (Brown et al. 2002). Recent numerical modeling suggests that substantial amounts of glass can be formed by radiative/convective heating of the surface during larger, >100 Mt low-altitude airbursts (Boslough and Crawford 2008), supporting earlier suggestions that the Libyan Desert Glass and the Muong-Nong Tektites of southeast Asia may have formed from such events (Wasson 2003).

Thus, there is growing evidence to suggest that airbursts—and the glass produced by such events—should occur more frequently than has been previously recognized in the geological record. This raises the possibility that prehistoric populations may have experienced the effects of such impact events. Despite this and until recently, there has been little consideration of, or search for evidence of, impact airbursts and small impact cratering events in the geological record. Complications arise because many of these recent impacts may have only penetrated surficial, unconsolidated sediments. Current classification schemes for shock metamorphic effects in rock-forming minerals are generally only typically available for dense, non-porous crystalline rocks (Stöffler 1971). Studies of sandstones from Barringer (Meteor) Crater (Kieffer et al. 1976) and the Haughton structure (Osinski 2007) indicate that similar shock metamorphic effects (e.g., shatter cones, PDFs, diaplectic glass, lechatelierite) do form in quartz in sedimentary targets, although the pressures and temperatures required to form these features are substantially lower. Recent work has also resulted in an increased—although still incomplete—understanding of shock effects in carbonates (see Osinski et al. 2008 and references therein). Relatively little is known, however, about the products of impacts into unconsolidated sedimentary rocks and soils and whether any of the characteristic shock metamorphic effects—such as planar deformation features (PDFs) and diaplectic glass—will form in significant quantities.

In this study, we report on unusual silicate glass—Dakhleh Glass (DG)—from the Dakhleh Oasis, Western Desert, Egypt. This glass, which has been dated at $\sim 120 \pm 40$ ka using stratigraphic and radiometric techniques (Kleindienst

et al. 2006; Blackwell et al. 2008; Schwarcz et al. Forthcoming), has previously been interpreted as the product of impact melting (Osinski et al. 2007). Here, we present observations made during fieldwork in January–February 2007 and new analytical studies. This work suggests that the DG formed from an impact event into, or above, an unconsolidated sedimentary target. We also draw upon recent work on airbursts (Boslough and Crawford 2008) to suggest that the properties of Dakhleh Glass, coupled with the apparent absence of a crater, can best be explained by radiative and convective melting of surficial sediments as a result of a large airburst event.

GEOLOGICAL AND ARCHAEOLOGICAL SETTING OF THE DAKHLEH OASIS

The Dakhleh Oasis is one of 5 major oases in the Western Desert of Egypt. This region preserves a rich history of habitation stretching back over 400,000 years before the emergence of *Homo sapiens* (Churcher and Mills 1999; Kleindienst 1999). In this time, the region has undergone repeated major environmental changes; today conditions are hyper-arid. At the time of impact, it is likely that Middle Stone Age people inhabited the Dakhleh Oasis (Kleindienst et al. 2006; Smith et al. 2009); geoarchaeological evidence suggests that this region comprised extensive wetlands and/or lakes, providing human inhabitants with abundant faunal and floral resources, even when much of the surrounding desert may have been largely uninhabited (Kieniewicz and Smith 2009).

The Dakhleh Oasis is situated within a ~ 2000 km² wind-ablated, stratigraphically-controlled, depression in the Western Desert of Egypt (Figs. 1 and 2). This region, located south of the Libyan Plateau, comprises a series of Cretaceous to Eocene sedimentary rocks consisting of predominantly sandstones, limestones, and shales, with minor siltstones and phosphatic horizons. These lithologies are unconformably overlain by a series of Pleistocene fluvial, lacustrine, paludal, and spring sediments, deposited principally during periodic pluvial (humid) phases (Churcher et al. 1999; Kleindienst et al. 1999; Kieniewicz and Smith 2009). In the lowlands, Pleistocene lacustrine and shoreline sediments predominate: they are typically lacustrine calcareous silty sediments (CSS), occurring primarily as erosional remnants along the margins of the modern oasis (Figs. 1 and 2).

FIELD OBSERVATIONS

Dakhleh Glass

Dakhleh Glass was first observed during regional archaeological and palaeoenvironmental surveys in the 1980s and 1990s (Kleindienst et al. 2006), with 6 known occurrences (Osinski et al. 2007). In 2007, we carried out a

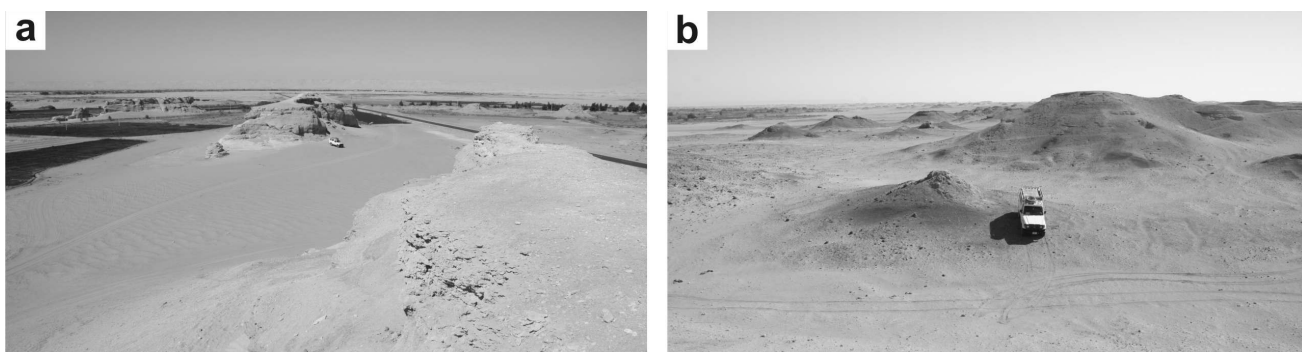


Fig. 1. Panoramic overview images of the Dakhleh Oasis. a) Image taken at the eastern edge of the oasis looking north with the Libyan Plateau in the background. Pleistocene lacustrine sediments (CSS) are located as erosional remnants on mesas of Taref Formation sandstone. b) Image looking east, taken in the central part of the oasis, showing erosional remnants of Pleistocene lacustrine sediments (CSS).

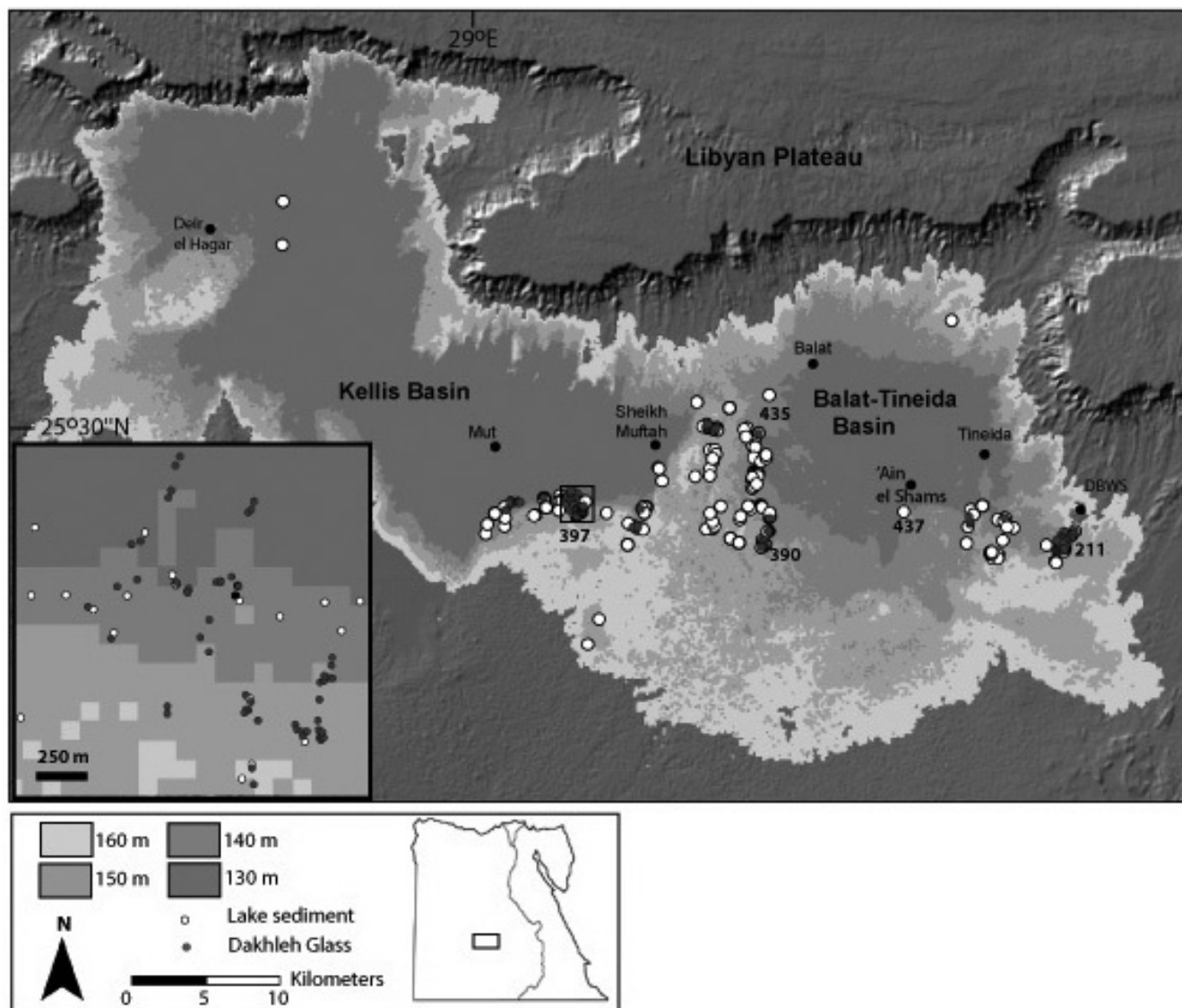


Fig. 2. a) ASTER image of the Dakhleh Oasis. b) Location of Dakhleh Glass and Pleistocene lacustrine sediments within the Dakhleh Oasis, Western Desert, Egypt (see inset for location in Egypt). The contours represent projected extents of the paleolake (s) within which the lacustrine sediments were deposited.

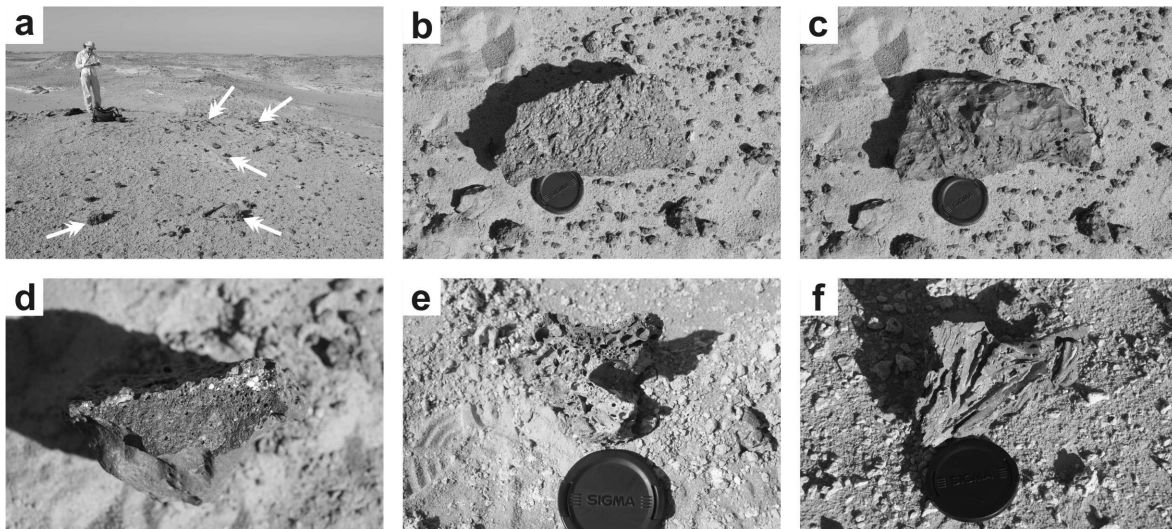


Fig. 3. Field images of DG lag deposits. a) Area of abundant DG lagged on the surface of Pleistocene lacustrine sediments; the arrows point to some large DG specimens. b) Upper surfaces of many large DG lag samples appear to be in place and are highly vesiculated. This contrasts with the smooth, irregular lower surfaces (c). 7 cm lens cap for scale. d) In cross-section, it is clear that there is an increase in the number of vesicles towards the upper surface. Together, these features are indicative of ponding of melt and volatile loss through vesiculation. e) Highly vesicular pumice-like DG sample. 7 cm lens cap for scale. f) Plant impressions on the underside of a DG sample. 7 cm lens cap for scale.

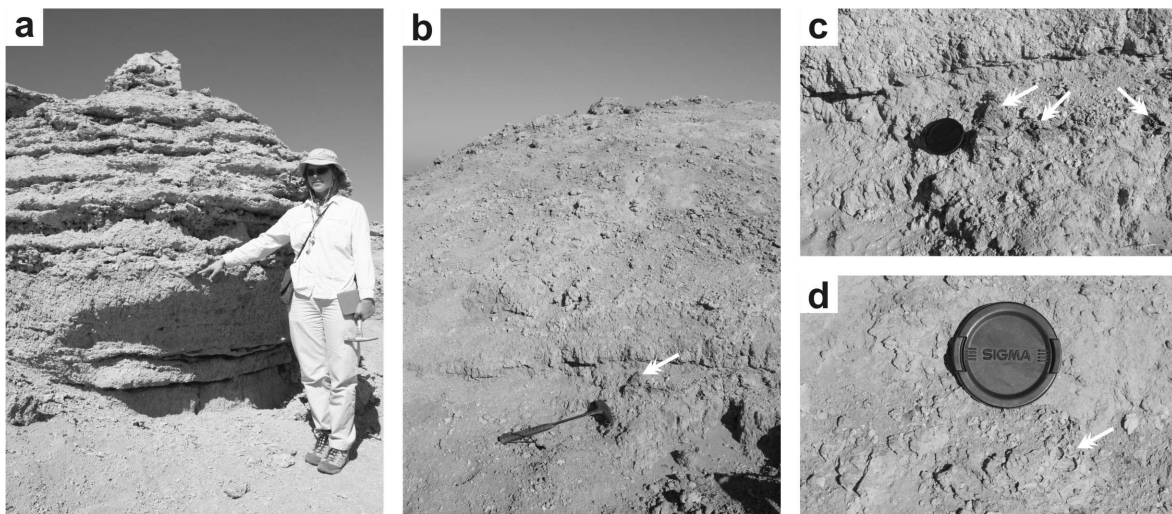


Fig. 4. Field images of DG in situ within Pleistocene lacustrine sediments. a) JK points to the DG-bearing layer within the lacustrine sediments. b) Arrow points to a dm-size DG fragment (35 cm) for scale. c) Close-up of (b). In situ DG specimens are typically cm-size and highly vesicular; arrows point to DG fragments. 7 cm lens cap for scale. d) Close-up image showing a highly vesiculated DG clast. 7 cm lens cap for scale.

systematic search and discovered DG at ~140 different locations throughout the Dakhleh Oasis, covering an area of $\sim 40 \times 10$ km (Fig. 1; a list of glass localities and samples is available on request from the primary author). Based on this new work, it is clear that DG occurs in 4 main settings: (1) as a lag deposit on the deflated surfaces of Pleistocene lacustrine CSS (Fig. 3); (2) in situ within the same sediments (Fig. 4); (3) as lag deposits on Taref Formation sandstone surfaces in close proximity to the Pleistocene lacustrine sediments, but in areas where these sediments have been completely removed (e.g., Fig. 3a); and (4) redeposited on, or into, Holocene pan

sediments. Searches of both older Quaternary formations and younger alluvial terraces yielded no DG fragments. Thus, an important observation is that the DG glass appears to be spatially associated with Middle Pleistocene lacustrine sediments. Recent fieldwork shows that these sediments were deposited in a lake(s) with a maximum estimated extent of ~ 1735 km² (Fig. 2b) (Kieniewicz and Smith 2009). Thus, the original areal extent of DG may have been much more than the current ~ 400 km².

DG is typically black when fresh and greenish-grey when weathered (Osinski et al. 2007). Our new field observations

indicate that individual specimens of DG vary markedly in terms of vesicularity (e.g., compare Figs. 3b and 3e), which is often a reflection of the size of the individual specimens. Smaller samples are typically highly vesicular (Fig. 3e); whereas larger masses, up to several kg and 30–40 cm across, are partially to fully crystalline (Figs. 3b–d). The majority of the large masses are flattened. Several of these flattened masses possess irregular but moulded lower surfaces and flat, vesicular upper surfaces, with an increase in vesiculation upwards (Figs. 3b–d). This gradient in vesicularity represents a clear way up criteria and suggests that these larger samples ponded in small topographic depressions with enough time to crystallize and release a volatile component. Many of the larger pieces are whole masses and not fragments broken from larger blocks (e.g., Fig. 3b) consistent with lack of significant movement/erosion following deposition. As noted previously, an unusual characteristic of the DG is that approximately one-third of DG specimens studied display impressions or “pyromorphs” of reed-like stems or leaves on the underside—or more rarely on other surfaces or internally—of the large flattened masses (Fig. 3f) (Osinski et al. 2007).

Host Sediments

As noted above, DG has been found in situ within Pleistocene CSS of lacustrine origin (Fig. 3). It is notable that sediments associated with the in situ DG, although chemically similar to the underlying lacustrine sediments, are reddened and occasionally contain charcoal and silicified organic matter, which are suggestive of burning. This is also consistent with the discovery of maghemite in association with the in situ glass (Kieniewicz 2007), which has been documented in goethite-rich soils that experienced burning (Grogan et al. 2003). These “burned” sediments often occur in discontinuous lenses in the stratigraphy immediately above the DG in the western, Kellis Basin, and have also been documented in the eastern Teneida Basin, suggesting that fires across the Dakhleh Oasis region may have been a significant feature of the aftermath of the glass-forming event (Kieniewicz 2007), implying the existence of moderately dense vegetation. Dewatering structures consistent with rapid deposition of sediment, as well as those that exhibit evidence for reworking, suggest that sediments may have been transported and redeposited from elsewhere in the basin.

ANALYTICAL TECHNIQUES

Several of us collected over 200 samples of DG and surrounding sedimentary lithologies over numerous field seasons in the Dakhleh Oasis. We performed optical microscopy on polished thin sections from 45 DG and 6 cultural glass samples. Quantitative analyses and investigation of micro-textures were then carried out using

wavelength dispersive X-ray (WDS) techniques on a JEOL JXA-8900 L electron microprobe. The beam operating conditions for the electron microprobe were 15 kV and 20 nA during analysis of glasses. The standards used consisted of natural and synthetic mineral and glass phases; the glass standard used was VG-568. Mobilization effects for alkali metals were reduced by using raster scan-modes over an area of $5 \times 5 \mu\text{m}$. Data were reduced using ZAF procedures incorporated into the operating systems. Back-scattered electron (BSE) imagery was used to investigate the micro-textures of the glasses. Approximately 165 analyses of DG and 40 analyses of cultural glasses were collected.

We determined the bulk chemistry of 20 samples of Dakhleh Glass and 6 samples of sediments and sedimentary rocks from the Dakhleh Oasis region were obtained using X-ray fluorescence (XRF) techniques. This augments the XRF analyses of 8 DG samples and 42 sedimentary lithologies presented in Osinski et al. (2007). Analyses were carried out on a PHILIPS PW2440 4kW automated XRF spectrometer system by Geochemical Laboratories, McGill University, Montreal, Canada. This system uses a rhodium 60kV end window X-ray tube, five X-ray detectors, four primary beam filters, eight analyzing crystals, two fixed channels for simultaneous measurement of Na and F, and PW2540 168 sample x-y autochanger. The major elements were analyzed using 32 mm diameter fused beads prepared from a 1:5 sample: lithium tetraborate mixture. Minor element analyses were performed on 40 mm diameter pressed pellets prepared from a mixture of 10g sample powder with 2 g Hoechst Wax C Micropowder.

PETROGRAPHY AND GEOCHEMISTRY OF THE DAKHLEH GLASS

The Dakhleh Glass comprises a highly vesicular, glassy groundmass containing primary crystallites (clinopyroxene, with minor plagioclase), spherules, and lithic and mineral clasts.

Glass

Optical and scanning electron microscopy observations mirror the field and hand specimen observations and show that the DG bodies vary markedly in terms of vesicularity (e.g., compare Figs. 3d, 3e, 5a, 5b, and 6a–c). Despite its name, the Dakhleh Glass is typically rich in crystallites (Fig. 5c). Hypohyaline (i.e., >80% glass) samples are rare (Fig. 5d) and hypocrySTALLINE samples (i.e., mixtures of glass and crystals) predominate (Figs. 5c, 5e, 5f) so that actual glass contents range from ~35 to 10 vol% (Osinski et al. 2007). Completely crystalline samples are also present but are rare. Such samples may, therefore, be best termed “clast-poor glassy impact melt rocks” or just “impact melt rocks” (Stöffler and Grieve 2007); however, we use the term Dakhleh

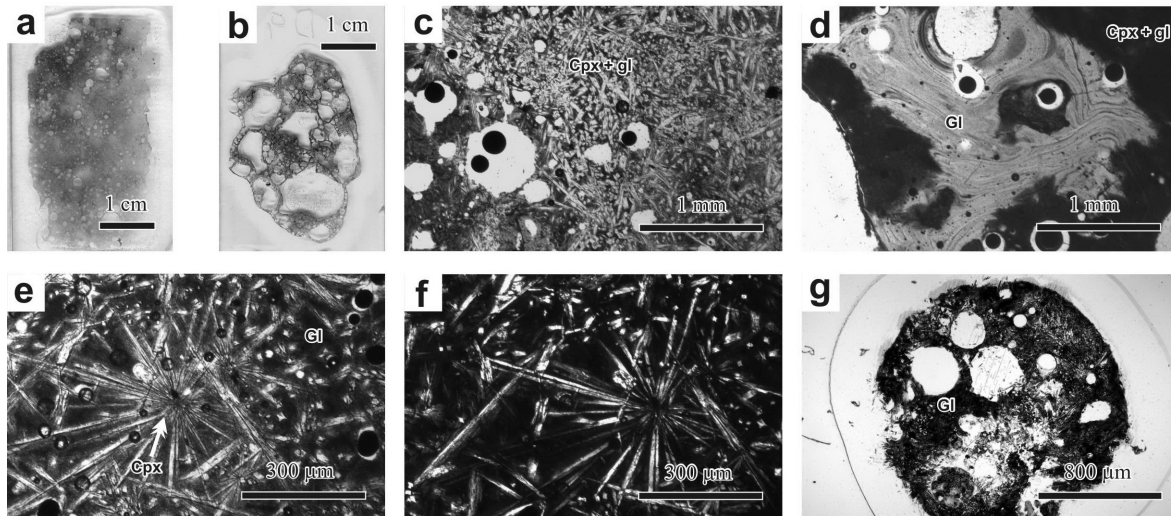


Fig. 5. a and b) Scanned polished thin section images showing the different degrees of vesicularity of the DG. The sample in (a) is from a large 20 cm size specimen; whereas the image in (b) shows the complete particle. d) Plane polarized light photomicrograph showing an enclave of transparent, crystallite-free glass (gl), within crystallite-rich darker glass (Cpx + gl). e and f) Plane and cross polarized light photomicrographs, respectively, showing relatively large clinopyroxene crystallites. g) Plane and polarized light photomicrograph of a glass spherule isolated from Pleistocene lacustrine sediments.

Glass here because this name has been associated with this material for over 25 years (Schwarcz et al., Forthcoming).

In thin section, crystallite-free glassy areas within DG glass samples are colorless and transparent (Fig. 5d). The bulk of the DG samples, however, have a grainy and “spotty” appearance. This dark coloration can be explained by the interaction of incident light with the crystallites, resulting in reduced light transmission through the sample. The majority of DG specimens investigated display evidence for flow in the form of elongated and irregularly-shaped vesicles (Figs. 6a and 6b) and intermingling of glasses of different composition (Figs. 7a–d).

X-Ray Fluorescence data for 24 individual samples of DG are presented in Table 1. Given the bulk nature of these analyses (i.e., it was not possible to completely separate clasts, spherules, globules, and secondary alteration products from the glass), the data should be interpreted with caution; however, these analyses are useful for assessing the major geochemical properties of the DG. It is notable that the DG is typically CaO- and Al₂O₃-rich, although there are considerable variations (e.g., from 8 to 21 wt% CaO) between individual samples and between different locations (Table 1). There is no systematic difference in composition between DG found as a lag and that found in situ (Table 1). Alkalis are typically <2 wt%. Loss-on-ignition (LOI) data suggest the presence of variable amounts of volatiles (Table 1). Some of these volatiles are undoubtedly bound in secondary phases such as calcite caliche and anhydrite; however, the systematically low WDS totals (typically 97–100 wt%; see below) in several samples suggest that the relatively high volatile contents may be original. The lack of perlitic fractures—which form due to the accommodation of strain following volume increases associated with the diffusion of

meteoric water into a solid glass (Marshall 1961)—also suggests that these volatile contents may be original. This is consistent with the pristine condition of the DG and the current hyper arid environment.

Trace element data for DG show persistent amounts of Ni (up to 46 ppm), Co (up to 280 ppm), and Cr (up to 46 ppm); however, there is no systematic enrichment relative to values for regional geological units (compare Tables 1 and 2). It is notable that analyses of surficial present-day sediments from several locations show elevated Ni (up to 2063 ppm), Co (up to 1025 ppm) and Cr (up to 176 ppm) (Table 2).

Figure 8 shows Harker diagrams with individual WDS spot analyses for DG samples. Selected individual analyses of lagged and in situ DG samples are presented in Tables 3 and 4, respectively. WDS analyses confirm the XRF findings that DG is typically CaO- and Al₂O₃-rich. Glass areas adjacent to crystallites were avoided during WDS analyses. Element maps confirm that compositional variations in the glass due to crystal fractionation are only important immediately adjacent to the crystallites, such that variations in spot analyses within individual samples reflect actual variations in glass composition (Fig. 7). These data show that, including variations between DG samples from different locations in the Dakhleh Oasis and at single locations (Table 1), there are substantial internal compositional variations; the greatest deviation is in SiO₂, Al₂O₃, CaO and MgO contents (Figs. 7a–d and 8).

An important sub-type of DG occurs as small irregular-shaped enclaves of glass devoid of crystallites that appear darker, in BSE mode, than the ‘host’ glass (Fig. 6d). WDS analyses and element maps indicate that these irregular glasses are highly silica rich, with SiO₂ contents of ~90–100 wt% (Figs. 7q and 7r).

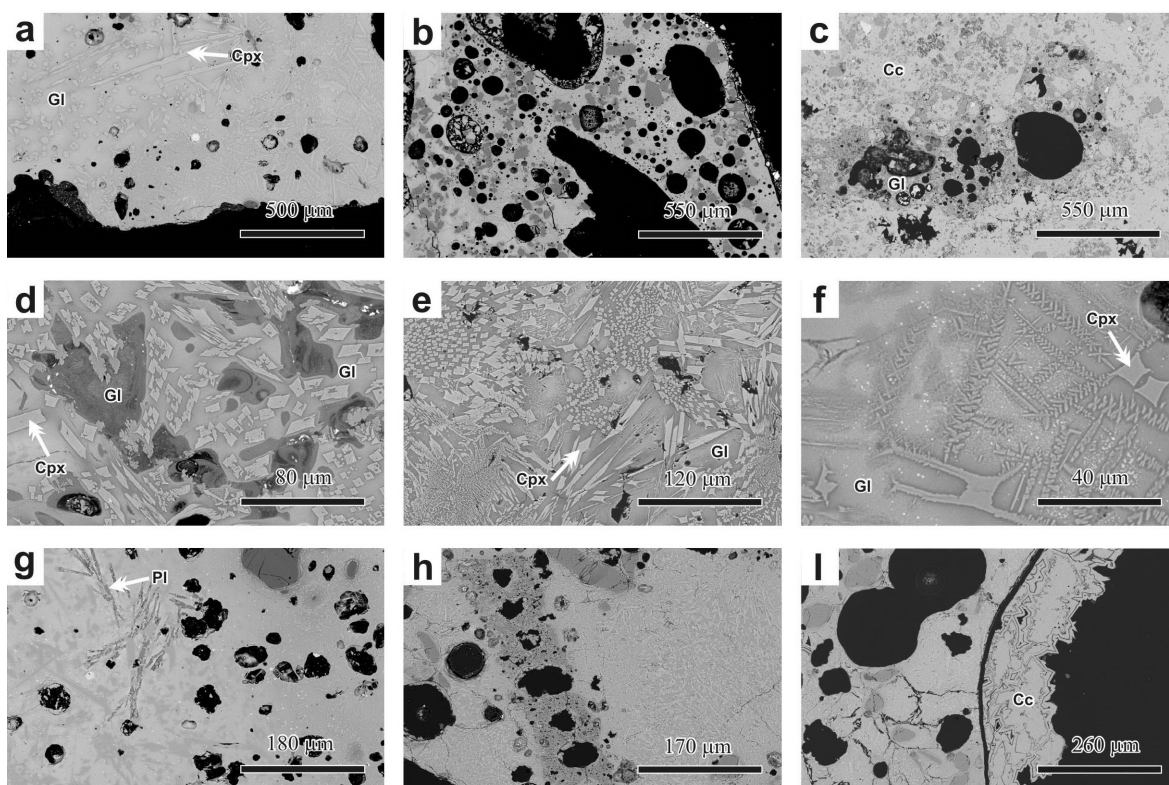


Fig. 6. Backscattered electron (BSE) photomicrographs of Dakhleh Glass. a and b) DG specimens can vary considerably in terms of their vesicularity, from vesicle-poor (a) to vesicle-rich (b). Clinopyroxene crystallites (Cpx) are typically abundant; glass (Gl) typically comprises <30 vol. c) In situ DG is typically highly vesicular. The clast in this image is enclosed in secondary calcite of the lacustrine sediments. d) Image showing irregular enclaves of pure SiO₂ glass, which appear darker in BSE mode than the surrounding host glass. e and f) Clinopyroxene is the dominant crystalline phase in DG glass, displaying a variety of spectacular crystal shapes dominated by skeletal morphologies indicative of rapid quenching. g) Plagioclase crystallites (Pl) in DG. h) Many DG specimens contain elongate clasts with aligned holes reminiscent of plant phytoliths (see text for details). i) Outer, broken vesicles of some DG samples may be filled with caliche that possesses a distinctive laminated texture.

Primary Crystallites

Clinopyroxene has previously been identified as the most common crystalline component of DG (Figs. 5c, 5e, 5f, and 6a, 6d–h; Osinski et al. 2007). This mineral displays a variety of crystal shapes (Figs. 6d–f), with skeletal morphologies predominating. Such morphologies are indicative of rapid crystallization from a melt due to high degrees of undercooling and supersaturation, as well as low nucleation densities (Donaldson 1976) and are common in impact-generated glasses (e.g., Hörz et al. 2002; Osinski 2003). Larger mm-size acicular and tabular crystals (e.g., Figs. 5e, 5f, 6d, 6e, and 7i–l) show some zonation, with Mg-rich cores (Fig. 7l). In addition, these large crystals can contain spherical and irregularly-shaped globules of FeS (Fig. 7j). The pyroxenes display varied compositions (En_{32.6–52.0}Fe_{0.3–13.7}Wo_{45.7–55.7}; Osinski et al. 2007). In the current study, we have also documented the presence of plagioclase crystallites in the DG for the first time (Figs. 6g and 7m–p). This identification is based mainly using element maps as the small size (typically <1 μm across) of the crystallites precluded an accurate determination of their composition.

Spherules

Spherules and globules of various phases are common in impactites (French 1998). In the DG, small (<5 μm in diameter) spherules of pyrrhotite (Figs. 5a, 5f, and 8i) and larger mm-sized spherules and irregularly shaped globules of calcite (Figs. 7q–t) are present. As noted above, pyrrhotite globules also occur within large clinopyroxene crystals. It is notable that the contact between the calcite globules and silicate glasses is always sharp, but often can be irregular with intermingling of the calcite and glass (Figs. 8q–t). The calcite globule morphology contrasts with the secondary calcareous and sulfate vesicle fills (Fig. 5i), which are common in the outer few mm of many of the glasses (Osinski et al. 2007). We have also identified individual spherules of DG in the Pleistocene lacustrine sediments (Fig. 5g).

Lithic and Mineral Clasts

Clasts of lithic and mineral debris are found in all samples, but typically comprise <5 vol% of individual DG samples. The most common clast type, found in all DG samples, are rounded

Table 1. X-ray fluorescence analyses of DG¹. Note that the samples are arranged in order from west to east across the Dakhleh Oasis. See Fig. 1 for location of basins (see Fig. 1).

Sample #	07-047	07-020	02-29 ²	07-013	07-040	07-025	07-047	DG-8	D11-DGC	02-34b ²	02-34b ²	07-042	07-037
Description	DG lag on deflated CSS surface	DG lag on Taref Fm. Surface	DG in situ in CSS	DG in situ in CSS	DG in situ in CSS	DG lag on eroded CSS slope	DG lag on deflated CSS surface	DG in situ in CSS	DG in situ in CSS	DG lag on eroded CSS surface	DG lag on eroded CSS surface	DG lag on Taref Fm. Surface	DG lag on eroded CSS surface
Geographic location	Kellis Basin	Kellis Basin	Kellis Basin	Kellis Basin	Kellis Basin	Kellis Basin	Kellis Basin	Kellis Basin	Kellis Basin	Kellis Basin	Kellis Basin	Kellis Basin	Kellis Basin
SiO ₂	70.68	56.11	56.74	61.73	56.63	54.52	70.68	62.0	57.3	58.28	56.43	56.50	55.65
TiO ₂	0.65	0.67	0.563	0.86	0.74	0.87	0.65	0.82	0.71	0.654	0.629	0.73	0.79
Al ₂ O ₃	10.98	10.31	8.37	12.46	12.07	11.60	10.98	10.6	11.0	9.99	9.64	11.52	11.74
Fe ₂ O ₃	3.98	3.53	3.75	6.16	5.00	5.01	3.98	5.38	4.30	4.06	4.03	4.46	5.18
MnO	0.07	0.07	0.071	0.12	0.09	0.09	0.07	0.10	0.09	0.092	0.089	0.08	0.09
MgO	1.53	7.19	4.62	3.25	3.49	5.47	1.53	4.04	4.79	5.33	5.83	4.38	3.21
CaO	7.27	16.81	12.36	8.91	11.99	17.24	7.27	10.47	12.29	12.05	12.85	12.65	12.75
Na ₂ O	0.60	2.50	3.64	2.64	3.42	2.18	0.60	2.3	4.4	3.95	4.04	2.64	2.21
K ₂ O	1.74	1.79	2.15	1.37	2.26	1.64	1.74	1.17	2.15	2.56	2.47	3.09	1.45
P ₂ O ₅	0.23	0.83	1.099	0.47	0.96	0.91	0.23	0.88	1.10	0.751	0.761	0.80	0.38
BaO	177	298	219	314	318	539	177	1.92	0.81	316	388	337	199
Ce	n.a	n.a	n.a	n.a	n.a	n.a	n.a	n.a	n.a	52	n.a	n.a	n.a
Co	40	15	<d/l	22	22	28	40	10.4	<8.8	<d/l	<d/l	21	43
Cr ₂ O ₃	139	132	143	194	169	179	139	131	113	151	144	165	238
Cu	n.a	n.a	n.a	n.a	n.a	n.a	n.a	n.a	n.a	39	n.a	n.a	n.a
Ni	29	19	29	45	39	41	29	n.a	n.a	27	27	27	46
Sc	n.a	n.a	n.a	n.a	n.a	n.a	n.a	n.a	n.a	15	n.a	n.a	n.a
V	n.a	n.a	n.a	n.a	n.a	n.a	n.a	n.a	n.a	90	n.a	n.a	n.a
Zn	n.a	n.a	n.a	n.a	n.a	n.a	n.a	n.a	n.a	<d/l	n.a	n.a	n.a
LOI	2.34	0.52	6.55	2.61	3.40	0.50	2.34	n.a	n.a	2.12	n.a	3.58	6.28
Total	100.12	100.37	99.95	100.63	100.10	100.11	100.12	97.77	98.17	99.91	96.77	100.48	99.77

Table 1. (Continued). X-ray fluorescence analyses of DG¹. Note that the samples are arranged in order from west to east across the Dakhleh Oasis. See Fig. 1 for location of basins (see Fig. 1).

Sample #	07-034	00-27b ²	07-024	07-054	07-044	07-046	07-007	07-053	00-28b ²	92bes6b ²	00-18b ²	00-18c ²	07-051
Description	DG lag on eroded CSS-FSS surface	DG lag on eroded CSS surface	DG lag on eroded CSS surface	DG lag on eroded CSS surface	DG lag on Taref Fm. Surface	DG lag on CSS-topped Taref Fm. gebel	DG lag on eroded CSSplanar surface	DG lag on eroded CSS surface	DG lag on eroded CSS surface	DG lag on eroded CSS surface	DG lag on eroded CSS surface	DG lag on eroded CSS surface	DG lag on eroded CSS surface
Geographic location	Kellis Basin	Balat Basin	Balat Basin	Balat Basin	Teneida Basin	Teneida Basin	Teneida Basin	Teneida Basin	Teneida Basin	Teneida Basin	Teneida Basin	Teneida Basin	Teneida Basin
SiO ₂	56.52	59.47	56.76	58.81	55.80	45.65	59.08	57.94	50.31	53.22	56.51	54.79	56.23
TiO ₂	0.75	0.747	0.66	0.621	0.96	0.68	0.68	0.617	0.507	0.500	0.531	0.516	0.44
Al ₂ O ₃	11.18	10.36	9.10	9.00	20.65	10.16	10.04	8.86	7.35	8.76	7.77	7.49	7.25
Fe ₂ O ₃	4.77	3.97	3.83	3.55	7.79	3.66	4.06	3.45	3.19	4.25	3.25	3.21	2.95
MnO	0.08	0.116	0.10	0.155	0.05	0.11	0.08	0.118	0.090	0.160	0.079	0.079	0.12
MgO	5.86	4.91	5.51	5.58	2.33	6.61	4.48	5.20	5.56	5.29	6.92	6.37	4.98
CaO	15.23	14.89	15.27	16.23	8.06	16.81	17.69	15.24	18.74	20.97	19.43	20.14	16.95
Na ₂ O	1.61	2.48	3.11	1.13	1.19	3.48	0.85	1.41	1.83	0.82	0.84	0.57	1.17
K ₂ O	2.34	1.60	1.81	2.76	1.99	1.65	1.41	3.30	2.20	1.39	1.71	1.52	2.14
P ₂ O ₅	0.70	0.448	0.61	1.281	0.50	0.64	0.84	0.902	1.005	1.220	1.171	1.075	1.03
BaO	309	337	302	267	180	2891	248	399	1005	n.a	251	310	345
Ce	n.a	51	n.a	n.a	n.a	n.a	n.a	n.a	47	n.a	45	28	n.a
Co	30	<d/l	22	27	30	17	22	25	11	n.a	<d/l	<d/l	19
Cr ₂ O ₃	144	152	127	122	279	115	140	112	102	n.a	130	103	125
Cu	n.a	27	n.a	n.a	n.a	n.a	n.a	n.a	41	n.a	37	37	n.a
Ni	36	29	27	27	40	17	35	24	26	n.a	28	28	17
Sc	n.a	15	n.a	n.a	n.a	n.a	n.a	n.a	11	n.a	15	13	n.a
V	n.a	96	n.a	n.a	n.a	n.a	n.a	n.a	66	n.a	71	68	n.a
Zn	n.a	<d/l	n.a	n.a	n.a	n.a	n.a	n.a	<d/l	n.a	<d/l	<d/l	n.a
LOI	0.72	0.97	3.02	0.83	0.85	9.84	0.79	2.73	9.21	n.a	1.85	4.11	6.31
Total	99.81	100.03	99.82	99.99	100.22	99.60	100.04	99.82	100.12	96.58	100.12	99.93	99.62

¹Data is in weight% for major elements and LOI and in ppm for trace elements (BaO and lower in the table). Detection limits are as follows (in ppm): SiO₂ (60); TiO₂ (35); Al₂O₃ (120); Fe₂O₃ (30); MnO (30); MgO (95); CaO (15); Na₂O (75); K₂O (25); P₂O₅ (35); BaO (17); Ce (15); Co (10); Cr₂O₃ (15); (2); Ni (3); Sc (10); V (10); Zn (2); LOI (100). Abbreviations: CSS = calcareous silty sediments; Fm. = Formation; n.a. = element not analyzed; <d/l = element below detection limit.

²Data from Osinski et al. (2007).

Table 2. Selected X-ray fluorescence analyses of sedimentary rocks and surficial sediments from the Dakhleh Oasis region.¹

Sample # Lithology Formation	RDR-SI ¹²		04-11c ²		04-30 ²		JM ²		TN ²		Q2 ²		390E		D8		D8 ash		D8 UGS1		390E		04-JRS		07-008				
	Sst Taref	Sst Mut	Sst Mut	Marl Mut	Shale Dakhla	Lst Tarawan	Lst Duwi	Silt Dakhla	Lst Tarawan	Lst Tarawan	Lst Duwi	Silt Dakhla	Silt Dakhla	Silt Dakhla	Silt Dakhla	Silt Dakhla	Silt Dakhla	Silt Dakhla	Silt Dakhla	Silt Dakhla	Silt Dakhla	Silt Dakhla	Silt Dakhla	Silt Dakhla	Silt Dakhla	Silt Dakhla	Silt Dakhla	Silt Dakhla	
SiO ₂	96.83	88.07	88.07	30.74	45.54	0.42	0.72	45.54	0.42	0.42	0.72	0.72	25.06	47.83	61.86	58.43	24.09	52.74	52.74	52.74	52.74	52.74	52.74	52.74	52.74	52.74	52.74	52.74	
TiO ₂	0.24	0.35	0.35	0.47	0.98	0.02	0.02	0.98	0.02	0.02	0.02	0.02	0.36	0.54	0.55	0.65	0.36	0.78	0.78	0.78	0.78	0.78	0.78	0.78	0.78	0.78	0.78	0.78	
Al ₂ O ₃	0.28	0.45	0.45	7.90	22.11	0.22	0.31	22.11	0.22	0.22	0.31	0.31	4.72	8.42	8.21	10.19	4.55	13.04	13.04	13.04	13.04	13.04	13.04	13.04	13.04	13.04	13.04	13.04	
Fe ₂ O ₃	0.68	6.64	6.64	5.33	5.28	0.11	0.15	5.28	0.11	0.11	0.15	0.15	1.90	3.57	3.41	9.70	1.83	4.65	4.65	4.65	4.65	4.65	4.65	4.65	4.65	4.65	4.65	4.65	
MnO	0.01	1.18	1.18	0.38	0.01	0.01	0.01	0.01	0.01	0.01	0.01	0.01	0.16	0.07	0.16	0.04	0.16	2.66	2.66	2.66	2.66	2.66	2.66	2.66	2.66	2.66	2.66	2.66	
MgO	0.04	0.28	0.28	5.48	2.68	0.23	0.45	2.68	0.23	0.23	0.45	0.45	2.59	2.80	2.91	2.18	2.51	3.01	3.01	3.01	3.01	3.01	3.01	3.01	3.01	3.01	3.01	3.01	
CaO	0.66	0.56	0.56	7.15	0.60	55.04	54.10	0.60	55.04	55.04	54.10	54.10	31.37	11.32	7.28	2.09	31.54	0.53	0.53	0.53	0.53	0.53	0.53	0.53	0.53	0.53	0.53	0.53	
Na ₂ O	0.04	0.11	0.11	6.45	0.58	0.03	0.02	0.58	0.03	0.03	0.02	0.02	1.13	4.43	1.88	1.91	1.03	1.12	1.12	1.12	1.12	1.12	1.12	1.12	1.12	1.12	1.12	1.12	
K ₂ O	0.02	0.11	0.11	1.05	1.38	<d/l	<d/l	1.38	<d/l	<d/l	<d/l	<d/l	0.46	0.70	1.34	1.83	0.43	1.70	1.70	1.70	1.70	1.70	1.70	1.70	1.70	1.70	1.70	1.70	
P ₂ O ₅	0.02	0.14	0.14	0.20	0.13	0.04	0.07	0.13	0.04	0.04	0.07	0.07	0.14	0.52	1.80	0.11	0.13	0.26	0.26	0.26	0.26	0.26	0.26	0.26	0.26	0.26	0.26	0.26	
SO ₃	n.a	n.a	n.a	n.a	1.51	n.a	n.a	1.51	n.a	n.a	n.a	n.a	n.a	n.a	n.a	n.a	n.a	n.a	n.a	n.a	n.a	n.a	n.a	n.a	n.a	n.a	n.a	n.a	
BaO	<d/l	92	92	145	124	20	<d/l	124	20	20	<d/l	<d/l	89	511	332	168	79	259	259	259	259	259	259	259	259	259	259	259	
Ce	31	31	31	37	88	31	18	88	31	31	18	18	2	6	6	24	4	91	91	91	91	91	91	91	91	91	91	91	
Co	<d/l	52	52	<d/l	<d/l	<d/l	<d/l	<d/l	<d/l	<d/l	<d/l	<d/l	2	6	6	24	4	1025	1025	1025	1025	1025	1025	1025	1025	1025	1025	1025	
Cr ₂ O ₃	96	71	71	83	305	42	33	305	42	42	33	33	82	124	125	149	83	176	176	176	176	176	176	176	176	176	176	176	
Cu	6	2	2	10	33	25	29	33	25	25	29	29	22	30	42	59	19	15	15	15	15	15	15	15	15	15	15	15	
Ni	18	42	42	31	34	12	17	34	12	12	17	17	22	30	42	59	19	2063	2063	2063	2063	2063	2063	2063	2063	2063	2063	2063	
Sc	<d/l	<d/l	<d/l	13	22	<d/l	<d/l	22	<d/l	<d/l	<d/l	<d/l	15	511	332	168	79	15	15	15	15	15	15	15	15	15	15	15	
V	20	19	19	72	213	13	16	213	13	13	16	16	99.78	99.82	99.85	99.95	99.81	118	118	118	118	118	118	118	118	118	118	118	
Zn	<d/l	100	100	<d/l	54	<d/l	<d/l	54	<d/l	<d/l	<d/l	<d/l	31.87	19.55	10.40	12.78	33.16	440	440	440	440	440	440	440	440	440	440	440	
LOI	1.08	2.10	2.10	34.77	19.16	43.87	44.22	19.16	43.87	43.87	44.22	44.22	99.78	99.82	99.85	99.95	99.81	99.94	99.94	99.94	99.94	99.94	99.94	99.94	99.94	99.94	99.94	99.94	99.94
Total	99.92	99.96	99.96	99.96	100.05	99.99	100.08	100.05	99.99	99.99	100.08	100.08	99.78	99.82	99.85	99.95	99.81	99.94	99.94	99.94	99.94	99.94	99.94	99.94	99.94	99.94	99.94	99.94	99.94

¹Data is in weight% for major elements and LOI and in ppm for trace elements (BaO and lower in the table). Detection limits are as follows (in ppm): SiO₂ (60); TiO₂ (35); Al₂O₃ (120); Fe₂O₃ (30); MnO (30); MgO (95); CaO (15); Na₂O (75); K₂O (25); P₂O₅ (35); BaO (17); Ce (15); Co (10); Cr₂O₃ (15); Ni (3); Sc (10); V (10); Zn (2); LOI (100). Abbreviations: Sst = sandstone; Lst = limestone; CSS = calcareous silty sediments; Fm. = Formation; n.a. = element not analyzed; <d/l = element below detection limit.

²Data from Osinski et al. (2007).

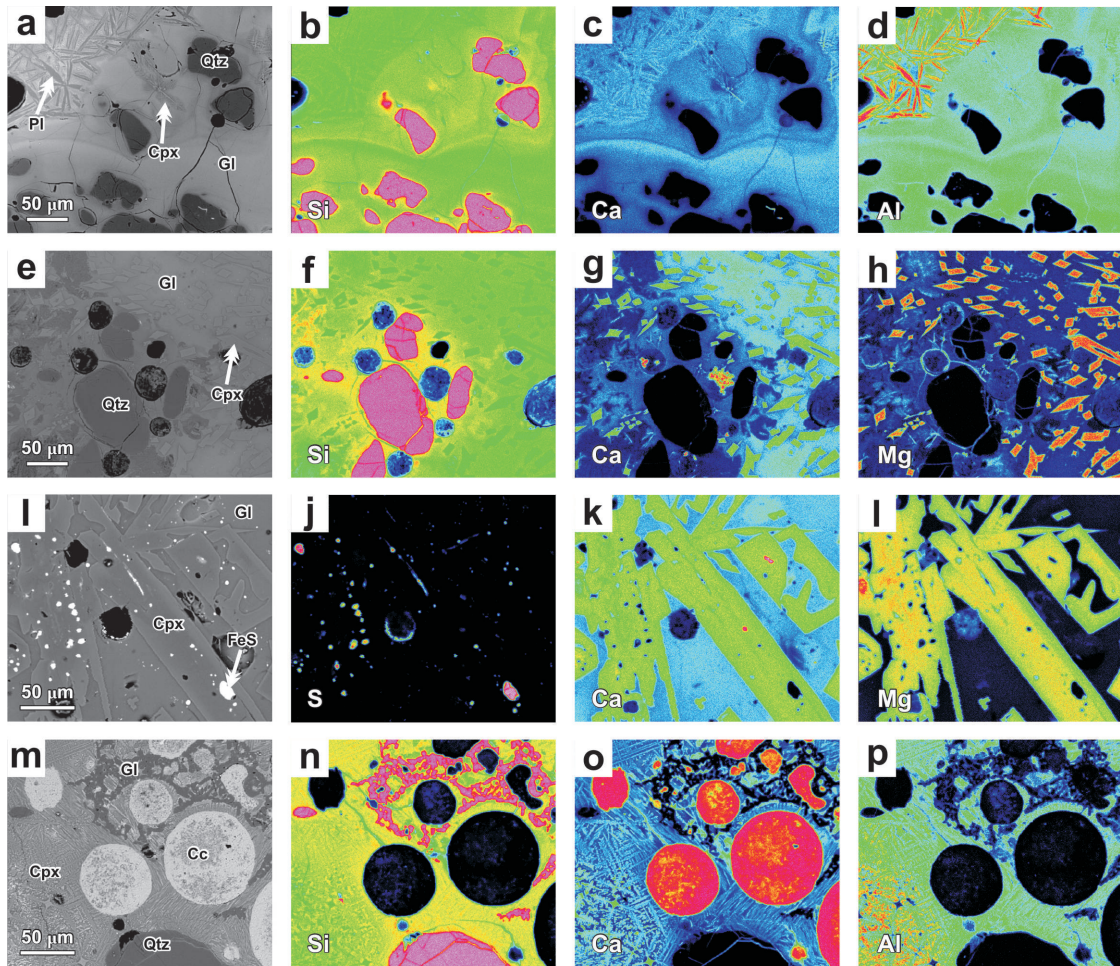


Fig. 7. Backscattered electron (BSE) photomicrographs (a, e, i, m) and element maps of DG. a–d) DG specimen with crystallite-rich and crystallite-free regions. Both plagioclase (Pl) and clinopyroxene (Cpx) crystallites are present. Flow-textures apparent in the BSE image (a) are confirmed in Si (b), Ca (c) and Al (d) element maps indicating incomplete mixing. Note the presence of rounded, fractured quartz grains. e–h) Some DG specimens display large internal variations in chemistry. Some of this is due to partial assimilation of quartz clasts—apparent as an enrichment of Si around the quartz grains in (b)—but other variations likely represent incomplete mixing of heterogeneous melts. These images show a Ca-rich region (right side of image) as exemplified in the Ca map (g); this region has subsequently crystallized more Ca-Mg-rich clinopyroxene crystallites. i–l) Immiscible spheres of pyrrhotite are present within the glass and clinopyroxene crystallites, as shown here. “Large” clinopyroxene crystallites such as these can show Mg-poor rims. m–p) Calcite melt spheres embedded in clinopyroxene-rich DG. Figures 7m–o are modified from Osinski et al. (2007). An irregular enclave of SiO₂ glass or lechatelierite is apparent in (n).

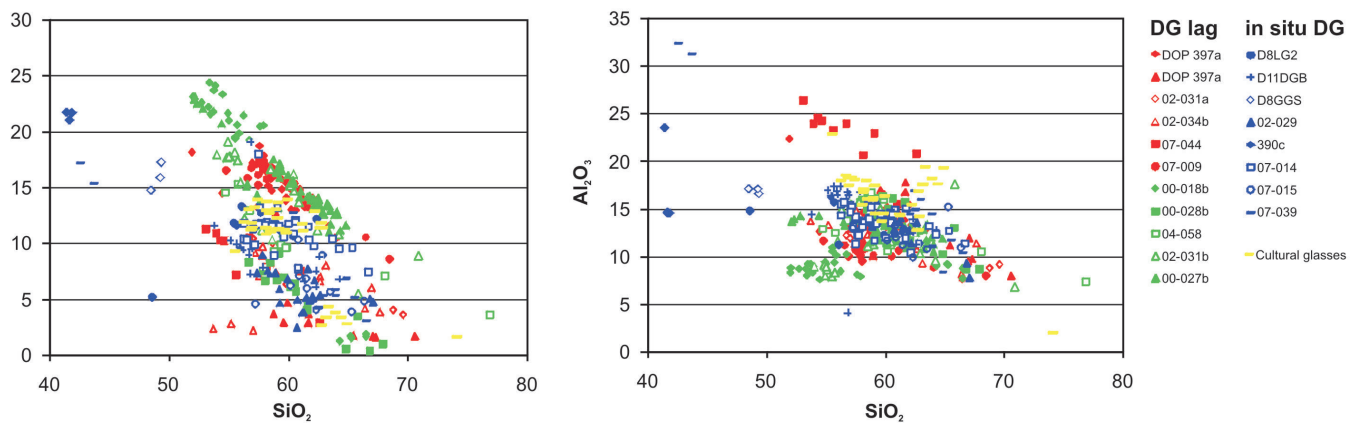


Fig. 8. Harker variation diagrams illustrating individual EDS/WDS analyses of the Dakhleh Glass.

to sub-rounded quartz grains ~0.1–0.8 mm in diameter (Figs. 6b and 7a, 7e, 7m). The amount of clastic material can range from <1 vol% (e.g., Fig. 6a) to ~10 vol% (e.g., Fig. 6b). There is no systematic variation with respect to geographic location in the Dakhleh Oasis, or between in situ and lagged samples. The quartz grains typically display irregular fractures (Figs. 7a, 7e, 7m); no planar features have been found to date. An unusual clast type can be seen in Fig. 6h. These elongate clasts comprise chains of circular holes, resemble cross sections of grass, sedge or reed leaves, and may represent recrystallized silica from phytoliths that retains some of its botanical structural organization; phytoliths are microscopic amorphous silicon dioxide ($\text{SiO}_2 \cdot \text{H}_2\text{O}$) particles that occur in various grasses (Piperno 2006). This is consistent with the presence of reed stem, root, and leaf casts in the CSS (Kieniewicz 2007). WDS analyses and element maps (not presented) confirm that these clasts are almost pure SiO_2 . Small (<2 cm diameter) angular fragments of fine-grained calcareous sedimentary rocks of unknown origin have been found in 3 samples.

DISCUSSION AND CONCLUSIONS

Origin of the Dakhleh Glass

The Dakhleh Glass, first discovered in the 1980's, is visually similar to many volcanic glasses. Osinski et al. (2007) interpreted these glasses as being the product of a meteorite impact event. This interpretation was based on two main properties of DG; namely, the unusual composition and the presence of SiO_2 glass enclaves (i.e., lechatelierite). The chemistry of DG (CaO and Al_2O_3 contents reach ~25 and ~18 wt%, respectively; Fig. 5; Table 1) and the lack of any documented Pleistocene-age volcanic features within several hundred km of the Dakhleh Oasis is inconsistent with a volcanic origin. The presence of lechatelierite—which forms at temperatures >1700 °C (Grieve et al. 1996)—as schlieren and enclaves within the DG, is incompatible with formation of DG via the burning of vegetation as surface soil temperatures following forest fires rarely exceed a few hundred °C (typically <600 °C) (Gimeno-Garcia et al. 2004), with temperatures of >100 °C rare at depths exceeding 0.5 cm (Auld and Bradstock 1996). Other evidence for an impact origin reported by Osinski et al. (2007) includes the presence of immiscible globules and spherules of pyrrhotite and calcite.

During the current investigations, an origin as fulgurites (i.e., the product of lightning strikes) was considered; however, the abundance of the DG in the Dakhleh Oasis region and its spatial and temporal relationship with the lacustrine sediments is not consistent with such an origin. The morphology and composition of DG is also inconsistent with being fulgurites, particularly those of the Sahara and other dry deserts, which typically display a vertically penetrative tubular morphology and are almost pure SiO_2 (Navarro-Gonzalez et al. 2007).

During fieldwork in 2007, it became apparent that a variety of cultural (i.e., human-made) glasses can be found in the Dakhleh Oasis region, often closely spatially associated with DG; many of the cultural glasses bear some physical and chemical resemblance to DG. For the dated DG samples (see Osinski et al. 2007) and those found in situ within the Pleistocene lacustrine sediments, it is clear that the age rules out a cultural origin; however, for DG found as a lag deposit, we must consider such an origin. The majority of glass from archaeological contexts within Dakhleh Oasis comes from the Roman Period (1st–4th centuries CE). It is notable that Roman glasses from the Eastern Roman Empire typically have a consistent chemical composition (Brill 1988). The composition of Roman glasses from Egypt is less well known, although some data exists to allow comparisons. In general, they have the following composition: SiO_2 (60–70 wt%), Al_2O_3 (1–3 wt%), Na_2O (10–25 wt%), and CaO (2–12 wt%); all other elements are <2 wt% (Bimson and Freestone 1991; Nenna et al. 2005). It is clear that the figures for SiO_2 in DG (Tables 2 and 3) are similar to cultural glasses known in Egypt; however, the other major elements differ markedly from what one would expect to see in a cultural glass.

The analysis of the two samples of glassy cultural material from the sites of Kellis and Deir el-Hagar in the Dakhleh Oasis do provide similar results to that of the DG; although, these cultural glasses display substantially lower Na_2O contents (Fig. 8) These results can be explained by the fact that the material that was analyzed is a type of material often known as “clinker” (Eccleston 1998, 2006). This is generally thought to be part of the internal lining of kilns or furnaces that was vitrified during the process of repeated firings; in the Dakhleh Oasis region, this material is often found associated with pottery shards (Fig. 9a). Combined observations also show that these cultural glasses rarely contain pyroxene crystallites, are typically more vesicular, and display reddish and greenish colors in hand specimen (Figs. 9b–d). Based on the thin section analysis of various archaeological ceramic samples from Dakhleh, the temperatures of pottery kilns at Kellis and Deir el-Hagar are unlikely to have exceeded 1000 °C at this time (Eccleston 1998, 2006). It is suggested that the difference between the DG and these cultural glasses is probably due to their degree of heating, with the DG subjected to a much higher temperature. The presence of lechatelierite in DG would, therefore, seem to rule out industrial activity. Metallurgical slags are also found in the Dakhleh Oasis region; however, these are readily distinguishable from DG by the presence of iron silicates—primarily wüstite—fayalite, and iron nodules (Eccleston 2006).

In summary, the properties of DG indicate that it formed during an impact event. In addition to the evidence outlined above and previously (Osinski et al. 2007), new evidence includes:

Table 3. Selected WDS analyses (weight %) of lagged DG samples.

Sample #	07-09	07-09	07-09	07-09	07-09	07-09	07-09	07-09	07-09	07-09	07-34	07-34	07-34	07-34	07-44	07-44	07-44	07-44
Analysis #	2	6	8	10	12	14	17	20	27	7	9	13	19	27	2	3	7	8
SiO ₂	57.95	57.56	57.77	61.18	64.12	56.95	56.62	58.43	59.03	58.66	58.34	58.66	58.34	61.80	54.34	53.11	56.76	55.65
TiO ₂	0.71	0.76	0.65	0.73	0.43	0.75	0.73	0.89	0.87	0.88	0.93	0.88	0.93	0.83	1.00	0.88	0.80	1.45
Al ₂ O ₃	10.11	10.57	10.70	10.62	8.83	10.03	11.16	14.76	15.24	14.31	13.31	14.31	13.31	14.19	24.57	26.38	23.94	23.21
Fe ₂ O ₃	3.93	3.89	3.98	3.26	2.52	4.18	4.69	4.96	4.61	5.03	6.01	5.03	6.01	3.83	3.80	3.13	2.44	5.12
MnO	0.14	0.14	0.15	0.13	0.07	0.17	0.14	0.10	0.08	0.09	0.12	0.09	0.12	0.06	0.04	0.05	0.04	0.07
MgO	2.09	2.33	2.25	1.50	4.50	2.42	3.25	0.92	0.73	1.13	1.31	1.13	1.31	0.57	1.34	1.07	0.97	2.34
CaO	17.85	17.38	17.43	14.00	10.54	16.75	15.82	13.08	12.20	13.48	13.37	13.48	13.37	12.20	10.24	11.26	10.50	7.13
Na ₂ O	2.21	2.31	2.20	2.34	2.12	2.14	2.41	2.36	2.60	2.22	2.07	2.22	2.07	2.45	1.10	1.50	1.60	0.99
K ₂ O	2.76	2.89	2.96	3.53	3.54	2.98	3.20	.73	2.92	2.57	2.39	2.57	2.39	2.90	1.86	1.57	1.66	2.57
NiO	0.01	0.00	0.00	0.00	0.00	0.00	0.00	0.00	0.00	0.00	0.00	0.00	0.00	0.00	0.01	0.03	0.00	0.02
SO ₃	0.25	0.19	0.25	0.14	0.13	0.49	0.21	0.15	0.37	0.12	0.80	0.12	0.80	0.25	0.06	0.13	0.03	0.08
P ₂ O ₅	1.46	1.40	1.38	0.94	0.65	1.67	1.77	0.76	0.77	0.67	0.62	0.67	0.62	0.57	0.28	0.27	0.14	0.37
Total	99.46	99.41	99.71	98.36	97.45	98.52	99.99	99.13	99.42	99.17	99.26	99.17	99.26	99.64	98.65	99.38	98.88	99.00

Table 4. Selected WDS analyses (weight %) of in situ DG samples.

Sample #	07-14	07-14	07-14	07-14	07-14	07-15	07-15	07-39	07-39	07-39	07-39	07-39	D8- LG2	D8- LG2	D8- LG2	D11 DGB	D11 DGB	D11 DGB	D8 GGS	D8 GGS	D8 GGS
Analysis #	1	4	10	14	14	7	1	8	11	11	4	9	3	6	14	14	1	2	1	1	2
SiO ₂	57.51	61.72	57.33	60.83	60.86	63.55	60.44	58.53	43.77	43.77	60.47	60.47	57.75	53.80	56.19	64.31	49.38	49.30			
TiO ₂	0.73	0.67	0.88	0.81	0.70	0.82	0.88	1.08	0.29	0.29	0.86	0.86	0.85	0.92	0.89	0.70	1.33	1.25			
Al ₂ O ₃	11.31	11.91	13.14	14.91	13.20	10.76	14.95	15.72	31.33	31.33	13.63	12.24	14.39	17.30	17.30	12.73	16.52	17.03			
Fe ₂ O ₃	3.34	5.25	5.67	5.03	5.73	6.47	3.39	4.32	2.18	2.18	3.83	4.31	6.88	4.00	2.59	7.17	7.54	7.54			
MnO	0.12	0.09	0.11	0.12	0.07	0.10	0.08	0.07	0.02	0.02	0.05	0.12	0.27	0.10	0.13	0.14	0.14	0.15			
MgO	2.22	3.26	3.64	2.73	2.83	0.41	0.66	0.62	2.43	2.43	2.93	3.79	0.83	0.77	0.62	0.62	4.27	4.77			
CaO	18.03	11.47	11.68	7.79	10.34	6.68	12.76	7.12	15.36	15.36	10.66	12.76	11.59	9.41	6.80	17.25	15.88	15.88			
Na ₂ O	2.53	2.32	3.14	2.47	1.92	6.29	2.69	5.91	2.23	2.23	4.31	4.42	4.82	6.17	4.72	1.94	2.43	2.43			
K ₂ O	2.51	2.40	2.65	3.84	2.67	3.85	2.68	6.09	0.33	0.33	2.13	1.98	3.82	3.98	5.48	0.62	0.58	0.58			
NiO	0.02	0.00	0.00	0.01	0.00	0.03	0.00	0.03	0.00	0.00	0.00	0.00	0.03	0.06	0.00	0.00	0.03	0.00			
SO ₃	0.54	0.00	0.02	0.01	0.06	0.02	0.17	0.07	0.06	0.06	0.12	0.13	0.22	0.06	0.10	0.32	0.45	0.45			
P ₂ O ₅	1.36	0.53	0.87	0.68	0.60	0.52	0.55	0.40	0.24	0.24	0.34	0.87	1.42	0.60	0.30	0.64	0.40	0.40			
Total	100.22	99.63	99.09	99.23	98.96	99.48	99.25	99.97	98.22	98.22	99.33	99.25	99.00	99.48	98.48	99.63	98.88	99.79			

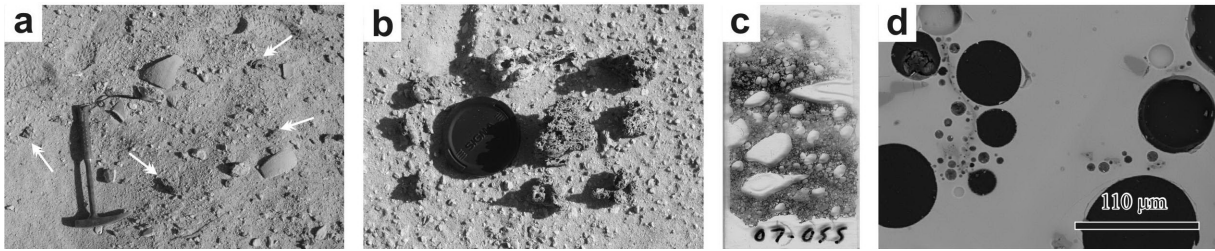


Fig. 9. Cultural glasses from the Dakhleh Oasis. a) Cultural glasses known as “clinker” are often found associated with pottery shards. Rock hammer for scale. b) Note the highly vesicular, frothy nature of the cultural glasses and their green color, which is in contrast to DG. 6 cm lens cap for scale. c) Scanned thin section image showing the green color of these cultural glasses. d) BSE SEM image of cultural glass showing the typical spherical vesicles and crystallite-free nature of these samples, in contrast to typical DG.

1. *Distribution and abundance*—The presence of abundant glass deposits over a region of ~ 400 km² and its spatial association with horizons within Pleistocene lacustrine sediments is best explained by the formation of the DG during a one-time catastrophic event. (It should be noted that the areal distribution of ~ 400 km² represents a minimum estimate; given the original distribution of lacustrine sediments of >1700 km², the original distribution of DG may have been considerable larger.)
2. *Shattered quartz*—Intensely fractured quartz grains are ubiquitous in DG. While not representing unequivocal shock metamorphic indicators, these shattered quartz grains are similar to those observed in the target rocks of the Libyan Desert Glass, which probably formed via meteorite impact (Kleinmann et al. 2001) or by an airburst associated with an impact (Boslough and Crawford 2008). Similar shattered quartz is also common at the BP and Oasis impact structures, Libya (French et al. 1974). Importantly, at Dakhleh, fractured quartz grains are only found in the Pleistocene lacustrine sediments, within which DG occurs (Kieniewicz 2007). A further possible explanation is that these quartz grains are not shattered from physical deformation, but that these effects are the result of rapid heating followed by slow cooling and the transformation to cristobalite or tridymite (Kieniewicz 2007).
3. *Glass spherules*—Spherules are commonplace in impact glasses. In addition to spheroids of pyrrhotite and calcite, we have also documented isolated glass spherules (Fig. 5g), which provides additional evidence for an impact melt origin of DG.
4. *Enriched Ni, Co and Cr contents*—Several samples of surficial present-day sediments show elevated Ni (up to 2063 ppm), Co (up to 1025 ppm) and Cr (up to 176 ppm) contents (Table 2). Meteoritic fragments have not been found to date in these samples, but the most reasonable explanation for such high Ni, Co and Cr contents would be the incorporation of a fine-grained projectile component into these sediments.
5. *Burnt sediments*—Recent work has shown that the Pleistocene lacustrine sediments surrounding DG are reddened and contain charcoal, silicified organic matter,

and maghemite (Kieniewicz 2007). This provides evidence for widespread burning of vegetation during the emplacement and deposition of the DG.

6. *Transport and emplacement*—The presence of plant impressions on the underside of many DG masses indicates that this melt landed on a solid surface in a semi-liquid state. This also requires the DG melt to have been generated at some distant point and to have then been transported to the site of emplacement; otherwise, it is difficult to envisage how some vegetation could have survived the temperatures associated with glass formation. These observations also suggest that DG was deposited in a variety of different settings; some wet, some dry, some with vegetation and some without.

Thus, the most plausible origin for the Dakhleh Glass is that it represents an impact-generated glass. Importantly, the large sizes of the DG pieces, the presence of appreciable amounts of volatiles, and the lack of aerodynamic shapes indicate that they are not, therefore, tektites (Koeberl 1994).

Melting from Shock Compression or Heating from a Large Aerial Burst?

Given the evidence for an impact origin for Dakhleh Glass, we now turn to the question of whether DG was generated during the formation of a hypervelocity impact crater or by a large airburst event. In terms of the size of crater required to generate such large masses of DG and to cover an area of 10×40 km, it is interesting to consider small simple craters (i.e., those less than ~ 2 – 4 km in diameter, depending on target lithology, in diameter on Earth). Studies at several well-documented simple craters, including Barringer Crater (Hörz et al. 2002), Lonar Crater (Fredriksson et al. 1973), and Wabar (Hörz et al. 1989), have long noted that impact melt is rare and is typically restricted to cm-size beads; although more recent work on the Wabar, Auouelloul, Henbury, and Lonar craters describes the presence of thin layers of melt as coatings around clasts, fragments of melt, and sometimes cm-thick accumulations (Newsom and Boslough 2008). Moreover, Barringer Crater is now understood to have been formed by a low velocity impactor that had already dissipated most of its energy in the atmosphere (Melosh and Collins

2005) and that event can be thought of as a low-altitude airburst that included a solid cratering-forming impact. If the DG did form from a hypervelocity impact crater then it would likely have been large enough (>4 km) to have a considerable ejecta blanket. However, despite over 25 years of field studies in the Dakhleh Oasis region by various researchers, no source crater or impact breccias (diagnostic of a proximal impact ejecta blanket) have been discovered to date. Given that only ~30 m of bedrock erosion occurred during the last 300 ka (Churcher and Kleindienst Forthcoming), it is unlikely that a crater of this size would have been completely eroded; other craters of this size, such as Flynn Creek, USA (apparent diameter 4 km), are still visible despite several 100 meters of erosion (Roddy 1979).

Therefore, in addition to conducting systematic surveys for DG in 2007, we also carried out investigations of candidate impact sites highlighted in remote sensing imagery (Haldemann et al. 2005) and from previous field studies (Kleindienst et al., Forthcoming). The first site was a small depression ~200 m across in the far western part of the Dakhleh Oasis (labelled "DBWS" in Fig. 2b); however, mapping suggests that the DBWS comprises arcuate ridges that may represent a fold basin structure and its size rules out an association with DG. We also visited the edge of a large ~3 km diameter circular depression, 'Ain el Shams, located in the central portion of the DG distribution pattern (Fig. 2). This feature is a salt pan and topographic low that acts as a sink for runoff from the surrounding irrigated fields. We found no evidence that this basin is an impact structure. If it were young impact crater, the evidence should be obvious. Shock metamorphic indicators and shattered quartz grains were absent in the sandstone on the southern edge of this feature. In addition, there is no evidence for an ejecta blanket.

The apparent lack of an impact crater or ejecta blanket suggests the possible origin of the DG through a large airburst event. But could such an event generate enough melt? Recent modeling indicates some key features of large airbursts (Boslough and Crawford 2008): during a low-altitude airburst, a high-temperature jet descends towards the surface and transfers its kinetic and internal energy to the atmosphere. Above a certain size threshold, this jet will make contact with the Earth's surface and expand radially outwards in the form of a fireball with temperatures exceeding the melting temperatures of silicate minerals; thus, surface materials can ablate by radiative or conductive heating, melt, and then rapidly quench to form glass. Importantly, for the most common incidence angle of 45°, a lateral component of the asteroid's initial momentum is transferred to the fireball so that it moves horizontally resulting in the area heated being many times larger than the diameter of the fireball itself. The melt can also be transported downrange for considerable distances and "collect in pools and form glass with larger dimensions" than the ablation depth (Boslough and Crawford 2008).

Numerical models designed to explain the origin of

Libyan Desert Glass are particularly informative. These ~28 Ma old glasses are found as cm-size masses (sometimes >20 cm across) distributed over an area of ~6500 km² in western Egypt (Weeks et al. 1984). With a composition of ~98 wt% SiO₂, it is clear that they were derived from the sandstone bedrock and surficial sands of this region. The numerical models used a 120 m diameter dunite sphere with an initial velocity of 20 km/s and a kinetic energy of 108 Mt (Boslough and Crawford 2008). In this scenario, the fireball makes contact with the surface over an area of >10 km diameter for >10 s and with temperatures >5000 °C. Thus, it would seem plausible that a similar-scale airburst could have formed the DG.

What can the composition of the Dakhleh Glass tell us about its origin? In earlier work (Osinski et al. 2007), we noted that the chemistry of the DG does not correlate with any individual formation within the Cretaceous to Eocene bedrocks underlying the Dakhleh Oasis. The DG could have been derived from a mixture of the Dakhla and Duwi Formations, part(s) of the underlying Mut and possibly Taref formations, and the overlying Pleistocene lacustrine sediments (Osinski et al. 2007). It is, however, possible to derive the DG glass from the Pleistocene lacustrine (CSS) sediments (compare Tables 1 and 2) as easily as it might be derived from Roman or modern superficial soils and erosional deposits, as both periods' unconsolidated deposits derive from the same series of bedrock strata. It is important to note that analysis of DG and their host sediments (e.g., see analyses of DG sample 07-007 and sediment sample 07-008, collected immediately underneath the DG sample) are never identical, which suggests some transport of the DG consistent with previous discussions and/or some limited mixing and homogenization of melts from discrete locations.

It is notable that DG is chemically heterogeneous, both within and between individual specimens (Tables 1, 3, and 4). We suggest that this is largely due to the effect of target lithology. It is clear from analyses of lithologies from the Dakhleh region that there is a large range of compositions for potential target rocks (Table 2). Thus, the initial shock melt would have varied in composition depending on the particular lithology melted, which would have been different across the Dakhleh Oasis. This can be seen on a regional scale in Table 1, where glasses in the easternmost Teneida Basin are generally more CaO-rich than glasses in the Kellis Basin, in the east. We do not know the exact stratigraphic level of the Pleistocene lacustrine sediments that would have been exposed at the time of impact, but a reasonable explanation for this east-west chemical gradient would be that DG was derived from more calcareous sediments in the Teneida Basin; whereas, in the Kellis Basin, more detrital quartz and clays may have been present.

In terms of intra-specimen chemical heterogeneity (e.g., see Tables 3 and 4), studies of impact melt products at structures in other heterogeneous sedimentary targets show

that homogenization of impact melts from such targets rarely occurs (Hörz et al. 2002; Osinski 2003). Element maps clearly show that this is also the case for DG (Figs. 8a–h). A subtle compositional feature of DG is also shown in Figs. 8b and 8f, where there is a slight enrichment of Si surrounding quartz clasts. Thus, a small component of the variation in SiO₂ contents of DG may reflect the minor assimilation of quartz clasts in the melt. Given the predominance of quartz grains as clasts, assimilation would not be expected to affect the variations in other major oxides.

In summary, numerical models of large airbursts (Boslough and Crawford 2008) would predict the following: 1) the formation of glass derived from surface materials; 2) distribution of glass over a large area; 3) the lack of a hypervelocity impact crater; 4) evidence for ponding and collection of melt. All of these predictions are consistent with observations of DG. An airburst origin also seems to account for the lack of unequivocal shock metamorphic indicators, which require relatively high shock pressures and, perhaps, coherent bedrock. Finally, we note that this is consistent with theoretical calculations and observations that have led to power-law size-frequency distribution curves (e.g., Harris 2008), suggesting that airbursts should occur relatively frequently throughout geological time. The glass produced by such events should also, therefore, be more common in the rock record than evidence for impact craters, assuming that the glass formed in a suitable preserving environment; the Western Desert of Egypt and the longstanding semiarid to hyper arid environment after the mid-Pleistocene is likely responsible for the relatively excellent preservation of DG.

Comparison with Other Enigmatic “Impact” Glasses

The production of glassy materials is a characteristic feature of meteorite impact events, with impact glasses being common in the proximal and distal ejecta deposits of many of the world's impact structures (Dressler and Reimold 2001). There is also a growing group of glasses either confirmed, or suspected, as being of impact origin but for which no source crater has been recognized; the DG falls into this category. Some of these glass occurrences are well known and widely accepted as being of impact origin (e.g., Libyan Desert Glass [Weeks et al. 1984]; Darwin Glass [Meisel et al. 1990]; urengoites or South Ural Glass [Deutsch et al. 1997]); others remain more enigmatic (Haines et al. 2001; Schultz et al. 2006). It is, however, important to make the distinction between tektites and impact glass. While the production of tektites is still not fully understood, it is widely thought that tektite melt is formed very early in the crater formation process from surficial sedimentary rocks and is ejected at high angles and high velocity into, and through, the atmosphere (Koeberl 1994); evidence for volatilization and reduction is also common. Tektites are characterized by aerodynamic shapes, extremely low volatile contents, and

general lack of clasts of target rock (Koeberl 1994). Some of these glasses are thought to represent tektites (Weeks et al. 1984; Deutsch et al. 1997; Glass and Koeberl 2006). Others, including DG, resemble impact glasses typically found in the proximal ejecta deposits of complex impact structures in that they display variable compositions, clasts of target rock, volatile contents of >0.1 wt%, and often considerable dimensions (up to dm in size). Notable examples include the Darwin and Edoewie glasses of Australia (Haines et al. 2001; Howard and Haines 2003) and the widespread glass occurrences in the Argentinean Pampas (Schultz et al. 2006), where more than one event has apparently occurred at the same locality over a multi-million-year history. As with the DG, these glasses also display similar compositions to the host sediments.

Based on our studies of DG coupled with the results of recent numerical modeling studies (Boslough and Crawford 2008) and the expected high frequency of airbursts (Brown et al. 2002), we suggest that many of these enigmatic impact glass occurrences—for which no craters have been identified—may be the result of airburst events.

Recognition of Impact Events into Unconsolidated Sedimentary Targets

The recognition of unequivocal shock metamorphic indicators from impacts into unconsolidated targets is a difficult and unresolved problem and one that has received relatively little attention to date. As noted at the outset of this manuscript, current classification schemes for shock metamorphic effects in rock-forming minerals have generally been developed for dense, non-porous crystalline rocks (Stöffler 1971), with schemes for sedimentary rocks only available for sandstones (Kieffer et al. 1976; Osinski 2007). The studies of Kieffer and colleagues (Kieffer et al. 1976) coupled with more recent numerical modeling (Wünnemann et al. 2008) clearly show that in the latter, a significant portion of the energy is consumed by collapsing pore spaces and compressing grain boundaries. An outcome of this is that energy is preferentially transferred into heat and melting of the target lithologies as opposed to forming shock metamorphic effects in minerals.

A review of the literature suggests that unequivocal shock metamorphic effects in minerals, such as PDFs and diaplectic glass, are generally absent at impact sites developed in unconsolidated sedimentary materials (e.g., Henbury [Taylor 1967; Ding and Veblen 2004]) and Wabar [Hörz et al. 1989; Shoemaker et al. 1997]); however, the lack of detailed studies leaves this question open. High-pressure polymorphs, such as coesite, have been documented from such impact sites (Chao et al. 1961). An additional unusual shock effect is “shock-lithification” and the production of “instant rock,” whereby unconsolidated quartz sands are compacted into coherent sandstone-like lithologies (Short 1966).

Interestingly, PDFs, whole rock glasses, and possible diaplectic glass have been documented at the Sedan nuclear test site (Short 1968); however, the production of shock metamorphic features at Sedan occurred primarily in blocks of coherent igneous rocks from within the alluvium so it is unclear whether this can be applied to a more typical finer-grained soil, sand, or lacustrine sediments as at Dakhleh. Possible PDFs in plagioclase and decorated PDFs in 6 quartz grains in impactites from Argentina derived from unconsolidated loess deposits (Schultz et al. 2006) suggest that shock metamorphic effects in such deposits may occur locally. The general lack of study complicates the recognition of impact events into unconsolidated targets and has resulted in considerable debate concerning the authenticity of several recent reports for young purported impact events where classic shock metamorphic indicators are lacking (Courty et al. 2008). Instead, evidence for impact in the form of “exotic micro-debris formed of filaments, flakes, spherules, beads, vesicular glass and angular clasts” has been proposed. It remains to be determined if such products are indicative of impacts into unconsolidated sedimentary target lithologies.

As noted above, intensely fractured quartz grains are ubiquitous in DG. We note that these shattered quartz grains are similar to those observed in the target rocks of the Libyan Desert Glass (Kleinmann et al. 2001) and the BP and Oasis impact structures, Libya (French et al. 1974). At Dakhleh, fractured quartz grains are only found in the DG and within the Pleistocene lacustrine sediments, within which DG occur (Kieniewicz 2007). Such shattered quartz grains may, therefore, provide supporting evidence of impacts into unconsolidated sedimentary targets, where much of the energy from the shock wave may go into pore collapse and displacement of grains rather than into the grains themselves.

In addition to shock metamorphic features, an obvious product of meteorite impact is the formation of glass. In the case of DG, the unique composition (i.e., CaO and Al₂O₃ contents up to ~25 and ~18 wt%, respectively) and abundance over such a wide area is inconsistent with a terrestrial origin such as volcanism, burning vegetation, or lightning strike; the age and composition similarly rules out a human origin. The same arguments can be, and have been, applied to other glasses with extremely high SiO₂ (Weeks et al. 1984; Deutsch et al. 1997). In other instances, glass compositions are similar to volcanic glasses (Schultz et al. 2006) such that this argument cannot be made.

Acknowledgments—We thank Anthony Mills, Director of the Dakhleh Oasis Project (DOP), and all DOP members for supporting many of the authors at the Dakhleh Oasis field sites and for their field observations. The primary author is supported by a Canadian Space Agency Space Science Fellowship and by a Discovery Grant from the Natural Sciences and Engineering Research Council of Canada

(NSERC). MRK acknowledges funding from the Social Sciences and Humanities Research Council of Canada, the University of Toronto, the National Geographic Society, and the Dakhleh Trust. JMK was supported by the Eugene Shoemaker Impact Cratering Award. We thank the reviewers, Abhijit Basu and Lutz Hecht, and the associate editor, John Spray, for their constructive comments that helped improve this manuscript.

Editorial Handling—Dr. John Spray

REFERENCES

- Auld T. D. and Bradstock R. A. 1996. Soil temperatures after the passage of a fire: Do they influence the germination of buried seeds? *Austral Ecology* 21:106–109.
- Bimson M. and Freestone I. 1991. Glassmaking on the Komasterion site: The discovery of an Islamic glass-making site in Middle Egypt. In *Excavations at el-Ashmunin IV: Hermopolis Magna: Buildings of the Roman Period*, edited by Bailey D. M. London: British Museum Press. pp. 64–65.
- Blackwell B. A. B., Long R. A., Kleindienst M. R., Churcher C. S., Smith J. R., Blickstein J. I. B., Kieniewicz J. M., and Adelsberger K. A. 2008. ESR analyses for herbivore teeth from Dakhleh Oasis, Egypt: Constraining pluvial events in the Western Desert. *Geological Society of America Abstracts with Programs* 40:386.
- Boslough M. B. and Crawford D. A. 1997. Shoemaker-Levy 9 and plume forming collisions on Earth. In *Near-Earth objects, Annals of the New York Academy of Sciences*, vol. 82, edited by Remo J. L. New York: New York Academy of Sciences. pp. 236–282.
- Boslough M. B. E. and Crawford D. A. 2008. Low-altitude airbursts and the impact threat. *International Journal of Impact Engineering*, doi:10.1016/j.ijimpeng.2008.07.053.
- Brill R. H. 1988. Scientific investigations of the Jalame Glass and related finds. In *Excavations at Jalame. Site of a glass factory in late Roman Palestine*, edited by Weinberg G. D. Columbia: University of Missouri Press. pp. 257–294.
- Brown P., Spalding R. E., ReVelle D. O., Tagliaferri E., and Worden S. P. 2002. The flux of small near-Earth objects colliding with the Earth. *Nature* 420:294–296.
- Chao E. C. T., Fahey J. J., and Littler J. 1961. Coesite from Wabar crater, near Al Hadida, Arabia. *Science* 133:882–883.
- Churcher C. S. and Mills A. J. 1999. Reports from the Survey of Dakhleh Oasis, Western Desert of Egypt, 1977–1987. Oxford: Oxbow Press. 271 p.
- Churcher C. S. and Kleindienst M. R. Forthcoming. Great Lakes in the Dakhleh Oasis: Mid-Pleistocene freshwater lakes in the Dakhleh Oasis depressions, Western Desert, Egypt. In *The Oasis papers IV and V*, edited by Leemhuis F. and Kaper O. Oxford: Oxbow Books.
- Churcher C. S., Kleindienst M. R., and Schwarcz H. P. 1999. Faunal remains from a Middle Pleistocene lacustrine marl in Dakhleh Oasis, Egypt: palaeoenvironmental reconstructions. *Palaeogeography, Palaeoclimatology, Palaeoecology* 154:301–312.
- Courty M. A., Deniaux B., Cortese G., Crisci A., Crosta X., Fedoroff F., Guichard F., Grice K., Greenwood P., Lavigne F., Mermoux M., Smith D. C., Peucker-Ehrenbrink B., Poitrasson B., Poreda R., Ravizza G., Thiemens M. H., Schärer U., Shukolyukov A., Walls M., and P. W. 2007. Evidence for trans-hemispheric dispersion of an ejecta debris-jet by a high-velocity tangential impact along the Austral-Indian Ocean at ca. 4 Kyr BP (abstract #8032). Bridging the Gap II: Effect of Target Properties on the Impact Cratering Process. CD-ROM.

- Deutsch A., Ostermann M., and Masaitis V. L. 1997. Geochemistry and neodymium-strontium isotope signature of tektite-like objects from Siberia (urengoites, South-Ural glass). *Meteoritics & Planetary Science* 32:679–686.
- Ding Y. and Veblen D. R. 2004. Impactite from Henbury, Australia. *American Mineralogist* 89:961–968.
- Donaldson C. H. 1976. An experimental investigation of olivine morphology. *Contributions to Mineralogy and Petrology* 57: 187–213.
- Dressler B. O. and Reimold W. U. 2001. Terrestrial impact melt rocks and glasses. *Earth Science Reviews* 56:205–284.
- Eccleston M. A. J. 1998. Petrographic study of locally produced ceramics from the Dakhleh Oasis, Egypt. M.Sc. thesis, University of Sheffield, Sheffield, UK.
- Eccleston M. A. J. 2006. Technological and social aspects of high-temperature industries in the Dakhleh Oasis, Egypt, during the Ptolemaic and Roman Periods. Ph.D. thesis, Monash University, Victoria, Australia.
- Fredriksson K., Dube A., Milton D. J., and Balasundaram M. S. 1973. Lonar Lake, India: An impact crater in basalt. *Science* 180:862–864.
- French B. M. 1998. *Traces of catastrophe. Handbook of shock-metamorphic effects in terrestrial meteorite impact structures*. Houston: Lunar and Planetary Institute. 120 p.
- French B. M., Underwood J. R., and Fisk E. P. 1974. Shock-metamorphic features in two meteorite impact structures, southeastern Libya. *Geological Society of America Bulletin* 85: 1425–1428.
- Gimeno-García E., Andreu V., and Rubio J. L. 2004. Spatial patterns of soil temperatures during experimental fires. *Geoderma* 118: 17–38.
- Glass B. P. and Koeberl C. 2006. Australasian microtektites and associated impact ejecta in the South China Sea and the Middle Pleistocene supereruption of Toba. *Meteoritics & Planetary Science* 41:305–326.
- Grieve R. A. F., Langenhorst F., and Stöffler D. 1996. Shock metamorphism of quartz in nature and experiment: II. Significance in geoscience. *Meteoritics & Planetary Science* 31: 6–35.
- Grogan K. L., Gilkes R. J., and Lottermoser B. G. 2003. Maghemite formation in burnt plant litter at East Trinity, North Queensland, Australia. *Clays and Clay Minerals* 51:390–396.
- Haines P. W., Jenkins R. J. F., and Kelley S. P. 2001. Pleistocene glass in the Australian desert: The case for an impact origin. *Geology* 29:899–902.
- Haldemann A. F. C., Kleindienst M. R., Churcher C. S., Smith J. R., Schwarcz H. P., and Osinski G. R. 2005. Volatiles in the desert: Subtle remote-sensing signatures of the Dakhleh Oasis catastrophic event, Western Desert, Egypt (abstract #3038). Role of Volatiles and Atmospheres on Martian Impact Craters. CD-ROM.
- Harris A. 2008. What Spaceguard did. *Nature* 453:1178–1179.
- Hörz F., See T. H., Murali A. V., and Blanchard D. P. 1989. Heterogeneous dissemination of projectile materials in the impact melts from Wabar crater, Saudi Arabia. Proceedings, 19th Lunar and Planetary Science Conference. pp. 697–709.
- Hörz F., Mittlefehldt D. W., See T. H., and Galindo C. 2002. Petrographic studies of the impact melts from Meteor Crater, Arizona, USA. *Meteoritics & Planetary Science* 37:501–531.
- Howard K. T. and Haines P. W. 2003. Distribution and abundance of Darwin impact glass (abstract #4057). 3rd International Conference on Large Meteorite Impacts. CD-ROM.
- Kieffer S. W., Phakey P. P., and Christie J. M. 1976. Shock processes in porous quartzite: Transmission electron microscope observations and theory. *Contributions to Mineralogy and Petrology* 59:41–93.
- Kieniewicz J. M. 2007. Pleistocene pluvial lakes of the Western Desert of Egypt: Paleoclimate, paleo hydrology, and paleolandscape reconstruction. Ph.D. thesis, Washington University, Missouri, USA.
- Kieniewicz J. M. and Smith J. R. 2009. Paleoenvironment and water balance of a Mid-Pleistocene pluvial lake, Dakhleh Oasis, Egypt. *Geological Society of America Bulletin*.
- Kleindienst M. R. 1999. Pleistocene archaeology and geoarchaeology of the Dakhleh Oasis: A status report. In *Reports from the survey of Dakhleh Oasis, Western Desert of Egypt, 1977–1987*, edited by Churcher C. S. and Mills A. J. Oxford: Oxbow Press. pp. 83–108.
- Kleindienst M. R., Churcher C. S., McDonald M. M. A., and Schwarcz H. 1999. Geography, geology, geochronology, and geoarchaeology of the Dakhleh Oasis region: An interim report. In *Reports from the survey of the Dakhleh Oasis, 1977–1987, Oxbow Monograph 99 Dakhleh Oasis Project Monograph 2*, edited by Churcher C. S. and Mills A. J. Oxford: Oxbow Press. pp. 1–54.
- Kleindienst M. R., Churcher C. S., Schwarcz H., and Haldemann A. F. C. Forthcoming. A Pleistocene catastrophic event at Dakhleh Oasis, Western Desert, Egypt. In *The Oasis Papers IV and V*, edited by Leemhuis F. and Kaper O. Oxford: Oxbow Books. In press.
- Kleindienst M. R., Churcher C. S., Churcher B., Schwarcz H. P., Haldemann A. F. C., Smith J. R., and Osinski G. R. 2006. Geoarchaeological investigations in Dakhleh Oasis, Desert, Egypt: Did a meteorite strike Dakhleh during the time of Middle Stone Age occupations? In *Archaeology of early Northeastern Africa: In memory of Lech Krzyżanika*, edited by Kroeper K., Chłodnicki M., and Kobusiewicz M. Poznań: Poznań Archaeological Museum.
- Kleinmann B., Horn P., and Langenhorst F. 2001. Evidence for shock metamorphism in sandstones from the Libyan Desert Glass strewn field. *Meteoritics & Planetary Science* 36:1277–1282.
- Koeberl C. 1994. Tektite origin by hypervelocity asteroidal or cometary impact: Target rocks, source craters, and mechanisms. In *Large meteorite impacts and planetary evolution*, edited by Dressler B. O., Grieve R. A. F., and Sharpton V. L. GSA Special Paper 293. Boulder: Geological Society of America. pp. 133–152.
- Marshall R. R. 1961. Devitrification of natural glass. *Geological Society of America Bulletin* 72:1493–1520.
- Masse W. B. 2007. The archaeology and anthropology of Quaternary period cosmic impact In *Comet/asteroid impacts and human society: An interdisciplinary approach*, edited by Bobrowsky P. T. and Rickman H. Berlin: Springer. pp. 25–70.
- Meisel T., Koeberl C., and Ford R. J. 1990. Geochemistry of Darwin impact glass and target rocks. *Geochimica et Cosmochimica Acta* 54:1463–1474.
- Melosh H. J. and Collins G. S. 2005. Meteor Crater formed by low-velocity impact. *Nature* 434:157.
- Navarro-Gonzalez R., Mahan S. A., Singhvi A. K., Navarro-Aceves R., Rajot J.-L., Mckay C. P., Coll P., and Raulin F. 2007. Paleocology reconstruction from trapped gases in a fulgurite from the late Pleistocene of the Libyan Desert. *Geology* 35:171–174.
- Nenna M.-D., Picon M., Thirion-Merle V. and Vichy M. 2005. Ateliers Primaries du Wadi Natrun: Nouvelles Découvertes. In *Annales du 16e Congrès de l'Association Internationale pour l'Histoire du Verre*. London. pp. 59–63.
- Newsom H. E. and Boslough M. B. E. 2008. Impact melt formation by low-altitude airburst processes, evidence from small terrestrial craters and numerical modeling (abstract #1460). 39th Lunar and Planetary Science Conference. CD-ROM.
- Osinski G. R. 2003. Impact glasses in fallout suevites from the Ries

- impact structure, Germany: An analytical SEM study. *Meteoritics & Planetary Science* 38:1641–1668.
- Osinski G. R. 2007. Impact metamorphism of CaCO₃-bearing sandstones at the Houghton structure, Canada. *Meteoritics & Planetary Science* 42:1945–1960.
- Osinski G. R., Grieve R. A. F., and Spray J. G. 2008. Impact melting in sedimentary target rocks: An assessment. In *The sedimentary record of meteorite impacts*, edited by Evans K. R., Horton W., King D. K. Jr., Morrow J. R., and Warne J. E. GSA Special Paper 437. Boulder: Geological Society of America. pp. 1–18.
- Osinski G. R., Schwarcz H. P., Smith J. R., Kleindienst M. R., Haldemann A. F. C., and Churcher C. S. 2007. Evidence for a ~200–100 ka meteorite impact in the Western Desert of Egypt. *Earth and Planetary Science Letters* 253:378–388.
- Piperno D. 2006. *Phytoliths: A comprehensive guide for archaeologists and paleogeologists*. New York: Altamira Press. 238 p.
- Roddy D. J. 1979. Structural deformation at the Flynn Creek impact crater, Tennessee: A preliminary report on deep drilling. Proceedings, 10th Lunar and Planetary Science Conference. pp. 2519–2534.
- Schultz P. H., Rate M., Hames W. E., Harris R. S., Bunch T. E., Koeberl C., Renne P., and Wittke J. 2006. The record of Miocene impacts in the Argentine Pampas. *Meteoritics & Planetary Science* 41:749–771.
- Schwarcz H. P., Szkudlarek R., Kleindienst M. R., and Evensen N. Forthcoming. Fire in the desert: The occurrence of a high-Ca silicate glass near the Dakhleh Oasis, Egypt. In *The Oasis Papers II*, edited by Wiseman M. Oxford: Oxbow Books.
- Shoemaker E. M. 1983. Asteroid and comet bombardment of the Earth. *Annual Review of Earth and Planetary Sciences* 11:461–494.
- Shoemaker E. M., Wynn J. C., Black D., and Blanchard D. 1997. Geology of the Wabar meteorite craters, Saudi Arabia. 28th Lunar and Planetary Science Conference. pp. 1313–1314.
- Short N. M. 1966. Shock-lithification of unconsolidated rock materials. *Science* 154:382–384.
- Short N. M. 1968. Nuclear-explosion-induced microdeformation of rocks: An aid to the recognition of meteorite impact structures. In *Shock metamorphism of natural materials*, edited by French B. M. and Short N. M. Baltimore: Mono Book Corporation. pp. 185–210.
- Smith J. R., Kleindienst M. R., Schwarcz H. P., Churcher C. S., Kieniewicz J. M., Osinski G. R., and Haldemann A. F. C. 2009. Potential consequences of a Mid-Pleistocene impact event for the Middle Stone Age occupants of Dakhleh Oasis, Western Desert, Egypt. *Quaternary Science Reviews* 195:138–149.
- Stöffler D. 1971. Progressive metamorphism and classification of shocked and brecciated crystalline rocks at impact craters. *Journal of Geophysical Research* 76:5541–5551.
- Stöffler D. and Grieve R. A. F. 2007. Impactites. In *Metamorphic rocks*, edited by Fettes D. and Desmons J. Cambridge: Cambridge University Press. pp. 82–92.
- Taylor S. R. 1967. Composition of meteorite impact glass across the Henbury strewn field. *Geochimica et Cosmochimica Acta* 31: 961–968.
- Vasilyev N. V. 1998. The Tunguska meteorite problem today. *Planetary and Space Science* 46:129–150.
- Wasson J. T. 2003. Large aerial bursts: An important class of terrestrial accretionary events. *Astrobiology* 3:163–179.
- Weeks R. A., Underwood J. R., and Giegengack R. 1984. Libyan desert glass: A review. *Journal of Non-Crystalline Solids* 67: 593–619.
- Wünnemann K., Collins G. S., and Osinski G. R. 2008. Numerical modelling of impact melt production on porous rocks. *Earth and Planetary Science Letters* 269:529–538.
-